


# Synthesis, recognition properties and drug release behavior of diltiazem-imprinted chitosan-based biomaterials

Kyeong-Jung Kim<sup>1</sup> | Ji-Hoon Kang<sup>1</sup> | Se-woon Choe<sup>2</sup> | Yeon-Hum Yun<sup>3</sup> |  
Soon-Do Yoon<sup>1</sup> 

<sup>1</sup>Department of Chemical and Biomolecular Engineering, Chonnam National University, Yeosu, Republic of Korea

<sup>2</sup>Department of IT Convergence Engineering, Kumoh National Institute of Technology, Gumi, Republic of Korea

<sup>3</sup>Engineering Research Institute, Chonnam National University, Gwangju, Republic of Korea

## Correspondence

Soon-Do Yoon, Department of Chemical and Biomolecular Engineering, Chonnam National University, Yeosu 59626, Republic of Korea.  
Email: [yunsd03@jnu.ac.kr](mailto:yunsd03@jnu.ac.kr)

## Funding information

Ministry of Education, Grant/Award Number: NRF- 2019R1I1A3A01061508

## Abstract

In this study, we prepared diltiazem (DTZ)-imprinted biomaterials for TDDS using chitosan, PVA, plasticizers, and sulfosuccinic acid. DTZ and the prepared biomaterials were characterized using field emission scanning electron microscopy, Fourier transform infrared, and <sup>1</sup>H nuclear magnetic resonance. DTZ recognition properties were confirmed by the binding isotherm, Scatchard plot analysis, the adsorption of materials with structures similar to DTZ, selectivity factor ( $\alpha$ ), and the imprinting-induced promotion of binding (IPB). Results revealed that adsorbed amount (Q) of DTZ-imprinted biomaterials was 1.63–2.53 times higher than that of non-imprinted biomaterials. In addition, it could be verified that DTZ-imprinted biomaterials have a binding site for DTZ according to Scatchard plot analysis. Furthermore, the results of  $\alpha$  and IPB indicated that the recognition capacity of the prepared DTZ-imprinted biomaterials is superior to that non-imprinted biomaterials. DTZ release properties were evaluated under various pH buffers and artificial skin. Results indicated that the DTZ release in buffers at low pH was faster than that in buffers at high pH. The DTZ release using artificial skin was continuous over 20 days. Furthermore, the DTZ release profile in the buffer followed the pseudo-Fickian diffusion mechanism, whereas the profile in the artificial skin test followed a non-Fickian diffusion mechanism.

## KEYWORDS

adsorption, biomaterials, drug delivery systems, polysaccharides, separation techniques

## 1 | INTRODUCTION

Transdermal drug delivery systems (TDDS) offer several advantages as an alternative to overcome the limitations of traditional drug delivery routes. TDDS can bypass the metabolic effects that reduce the bioavailability of drugs and can increase the duration of drug activity with

constant drug delivery. Moreover, the technique is non-invasive, eliminating problems such as medical waste and needle reuse. Owing to these advantages, in 1979, the first transdermal administration patch, the scopolamine patch, was approved in the U.S. Subsequently, various drug patches (including lidocaine, fentanyl, estradiol, clonidine, nitroglycerin, and testosterone) have been approved. The increasing prevalence of hypertension, angina, neurological disorders, and chronic pain owing to an aging society has led to the growth of the

Kyeong-Jung Kim, Ji-Hoon Kang, Se-woon Choe, and Yeon-Hum Yun contributed equally to this work.

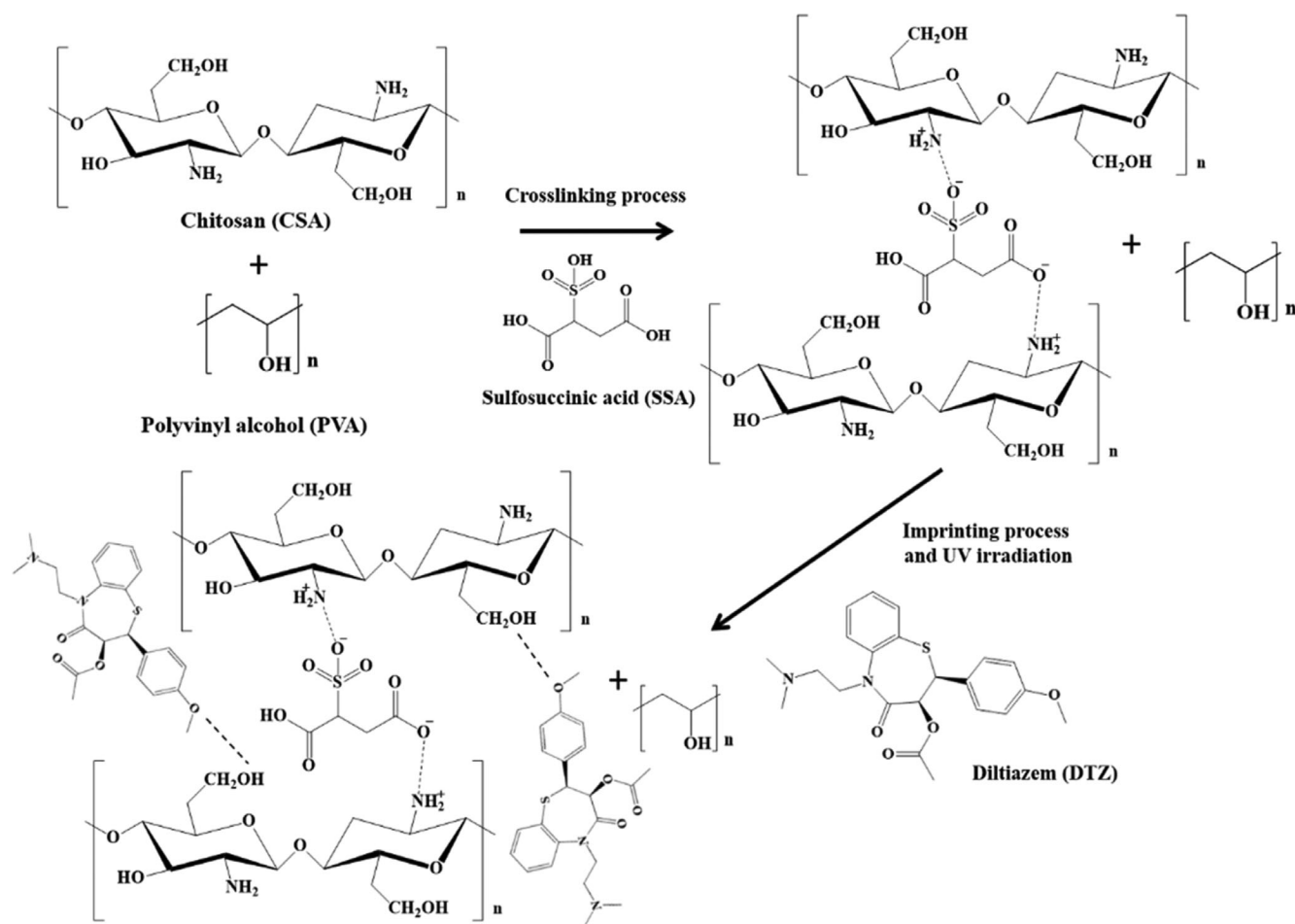
drug delivery market, and the global TDDS market is estimated to reach US \$ 9.6 billion by 2027. This market growth is mainly attributable to the improved bioavailability, high patient compliance, and continuous treatment offered by TDDS.<sup>1–4</sup>

Natural polymers, being inherently biocompatible and biodegradable, can be used as polymeric materials for TDDS. These include polysaccharides and proteins in general. Among these, chitosan (CSA) is a linear polysaccharide derived from the deacetylation of chitin and is composed of repeated N-acetyl-D-glucosamine units. CSA has been approved as “generally recognized as safe” (GRAS) by the US food and drug administration (FDA) for its biocompatibility, biodegradability, non-toxicity, and antibacterial properties.<sup>5,6</sup> Accordingly, it has been widely applied as an edible film, hemostatic agent, wound dressing, tissue engineering, and transporting pharmaceutical agents.<sup>7–9</sup> However, because CSA-based biomaterials have poor physical properties such as mechanical and water resistance properties, it is essential to improve their physical properties. Therefore, by blending two or more

polymers, their individual performance can be efficiently improved.

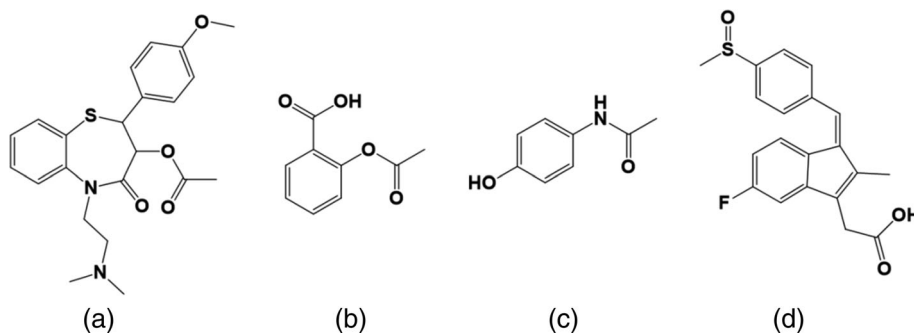
Polyvinyl alcohol (PVA) is inexpensive and has low cost, high biocompatibility, and film forming ability. In addition, the hydroxyl group in its molecular structure can form an intermolecular hydrogen bond with CSA to improve the physical properties of CSA-based biomaterials.<sup>10–12</sup> Another method to improve the performance of CSA-based biomaterials is the addition of chemical crosslinking agents. Sulfosuccinic acid (SSA) and glutaraldehyde are commonly used in this method. In our previous study, we reported that the addition of SSA and the UV irradiation process improved the mechanical properties, thermal properties, and water resistance of CSA/PVA blended films.<sup>13</sup> The crosslinking<sup>14</sup> and imprinting mechanisms are illustrated in Scheme 1. The imprinting for diltiazem (DTZ) as the target molecule used in present study generally reacts a hydrogen bonding, and the crosslinking for the prepared films is activated by UV irradiation.

DTZ, one of the calcium channel blockers, comprises benzothiazepines and is widely used in the treatment of



SCHEME 1 Crosslinking and imprinting mechanism for DTZ-imprinted CSA-based biomaterials.

**FIGURE 1** Chemical structures of the adsorption materials used in this study. (a) Diltiazem (DTZ), (b) aspirin (ASA), (c) acetaminophen (AAP), and (d) sulindac (SLD).



angina pectoris and hypertension. DTZ blocks the influx of calcium ions by binding to L-type calcium channels in cardiac smooth muscle cells. This leads to smooth muscle relaxation and vasodilation, resulting in a decrease in blood pressure.<sup>15,16</sup> Oral administration of DTZ reduces its bioavailability to 30–40% owing to the first-pass metabolism in the liver; it has a short biological half-life of 3.5 h. Overcoming these drawbacks requires high doses of DTZ to be frequently administered, thus necessitating different routes of DTZ delivery. Therefore, developing drug delivery formulations is essential to reduce administration frequency and dosage while maximizing treatment efficiency. In this study, DTZ was used as a target drug for TDDS.<sup>17,18</sup>

This study aimed to prepare DTZ-imprinted biomaterials using CSA, PVA, SSA, and plasticizers (glycerol (GL), and citric acid (CA)) for TDDS. Their physical properties, the recognition properties of DTZ, and DTZ profiles at various pH buffers and temperatures were investigated. The recognition properties were evaluated by binding isotherm, Scatchard plot analysis, the adsorption of materials with structures similar to DTZ such as aspirin (ASA), acetaminophen (AAP), and sulindac (SLD), selectivity factor ( $\alpha$ ), and the imprinting-induced promotion of binding (IPB). In addition, the drug release behavior of DTZ was investigated using Fickian diffusion and Korsmeyer-Peppas mechanisms as diffusion models. Furthermore, DTZ release properties were confirmed through an artificial skin test of the applicability of TDDS.

## 2 | MATERIALS AND METHODS

### 2.1 | Materials

Chitosan (CSA) (Mw: 500 kDa; the degree of deacetylation: 80%) and diltiazem hydrochloride (DTZ) were obtained from Tokyo Chemical Industry Co., Ltd. (Tokyo, Japan). Polyvinyl alcohol (PVA) (Mw: 89,000–98,000; the degree of hydrolysis: 99%), glycerol

(GL), citric acid (CA), lactic acid, sulfosuccinic acid (SSA), dimethyl sulfoxide (DMSO), aspirin (ASA), acetaminophen (AAP), and sulindac (SLD) were purchased from Sigma-Aldrich Chemical Company, Inc. (St. Louis, MO, USA). The chemical structures of DTA and similar structures, such as ASA, AAP, and SLD, are shown in Figure 1. All experiments used distilled deionized water (DW).

### 2.2 | Preparation of DTZ-imprinted CSA-based biomaterials

CSA and plasticizers (GL or CA) were dissolved in a 2% aqueous solution of lactic acid until a concentration of 2% (w/v) was achieved at 25.0°C. PVA solution was prepared by dissolving PVA in heated DW (95°C). These solutions were mixed and maintained at 95°C for 10 min. The mixture was blended using a mechanical stirrer (400 rpm) at room temperature for 60 min to obtain a homogeneous gel-like solution. After dissolving DTZ (0.5 g) as the target drug in DW, the DTZ solution was added dropwise for uniform recognition into a gel-like solution during the blending process. In addition, to evaluate the physical properties and recognition activity, CSA-based biomaterials without DTZ were prepared under same conditions. The components of prepared CSA-based biomaterials are summarized in Table 1. Bubbles were subsequently removed using an aspirator, and the gel-like solution was poured onto preheated Petri dishes (50°C,  $\Phi = 10$  cm). These Petri dishes were dried in a ventilated oven at 50°C for 24 h. These prepared CSA-based biomaterials were then irradiated by a UV lamp (OSRAM ULTRA VITALUX, 300 W) under atmospheric pressure.

### 2.3 | Physical properties

The water resistance properties of CSA-based biomaterials were evaluated by measuring their swelling behavior

TABLE 1 Composition of prepared CSA-based biomaterials.

Sample name	CSA (g)	PVA (g)	SSA (wt%)	GL (wt%)	CA (wt%)	DTZ (g)	DW (g)
CSAPS	2.0	2.0	20	—	—	—	160
CSAPSGL	2.0	2.0	20	40	—	—	160
CSAPSCA	2.0	2.0	20	—	40	—	160
CSAPSDTZ	2.0	2.0	20	—	—	0.5	180
CSAPSGLDTZ	2.0	2.0	20	40	—	0.5	180
CSAPSCADTZ	2.0	2.0	20	—	40	0.5	180

(SB) and solubility (S) with UV irradiation time. The prepared biomaterials were immersed in DW at 25.0°C. After 24 h, the moisture present on the surface of the biomaterials was removed and the weight of the biomaterials was measured. The SB of each biomaterial was calculated using the following equation (Equation (1)):

$$\text{Swelling behavior} = \frac{(W_e - W_0)}{W_0} \quad (1)$$

where  $W_e$  is the weight of the swollen biomaterials at equilibrium, and  $W_0$  is the initial weight of the dried biomaterials.

To remove the internal moisture, the swollen biomaterials were dried again at 50.0°C for 24 h. The S of each biomaterial was calculated using the following equation (Equation (2)):

$$\text{Solubility} = \frac{(W_0 - W_d)}{W_0} \quad (2)$$

where  $W_d$  is the dry weight of the swollen biomaterials, and  $W_0$  is the initial weight of the dry biomaterials.

The tensile strength (TS) and elongation at break (EB) of the biomaterials were analyzed using the Instron 6012 testing machine (Norwood, MA, USA). Six dumbbell-shaped specimens (ASTM D-412) were cut from the prepared biomaterials. Their thickness was measured three times using a mechanical scanner (digital thickness gauge “Mitutoyo” Tokyo, Japan) around the biomaterials; the average thickness was  $0.121 \pm 0.002$  mm. The gauge length and grip distance were both 50.0 mm. The crosshead speed was 20 mm/min, and the load cell was 250 kg. All samples were stored at 25°C and RH 55.0% for 1 week and then tested.

## 2.4 | Characterization

The morphologies of the CSA-based biomaterials with/without the addition of DTZ and plasticizers were analyzed via field emission scanning electron microscopy

(FE-SEM, ZEISS Sigma 500, Carl Zeiss Co., Ltd., Germany) at an acceleration voltage of 5.0 kV. Fourier transform infrared (FT-IR) spectroscopy of DTZ and the prepared biomaterials was performed using an FT-IR spectrophotometer (Spectrum Two, Perkin Elmer, USA). DTZ with/without UV irradiation was investigated using  $^1\text{H}$  nuclear magnetic resonance ( $^1\text{H}$  NMR) spectra.  $^1\text{H}$  NMR was recorded on a Varian Unity Inova 500 MHz spectrometer at the Korea Basic Science Institute (KBSI, Gwangju Center, Korea). Samples were dissolved in DMSO- $d_6$ .

## 2.5 | Recognition properties

To evaluate the recognition properties of the DTZ-imprinted CSA-based biomaterials, DTZ was extracted by the Soxhlet extraction method from DMSO over 28 h, and the biomaterials were alternately cleaned with DMSO and DW until DTZ was not detected by a UV-vis spectrophotometer (OPTIZEN 2120UV, Neogen, Co., Ltd., Korea). These biomaterials without DTZ were dried in a vacuum oven at 50°C for 12 h. Binding isotherms were obtained by adding a fixed biomaterial (ca. 0.1 g) into a 45 mL vial containing 30 mL of various initial DTZ concentrations (0.10–1.50  $\mu\text{mol/L}$ ). These vials were shaken in a shaking incubator (DS-210SF, Daewon Science, Inc., Korea) at 100 rpm and 25°C for 12 h until equilibrium was reached. To evaluate the DTZ recognition properties of non-imprinted CSA-based biomaterials, binding isotherm studies and the adsorption of materials with structures similar to DTZ were performed under the same conditions.

The adsorbed amount ( $Q$ ) of DTZ bound to the biomaterials was calculated using the following relationship (Equation (3)):

$$Q(\text{mmol/g}) = \frac{(C_i - C_e)V}{m} \quad (3)$$

where  $C_i$  and  $C_e$  are the initial and equilibrium concentrations of DTZ in the adsorption solution, respectively.

$V$  is the volume of the solution and  $m$  is the mass of the prepared biomaterials used. The binding affinity of the prepared biomaterials to DTZ was confirmed using Scatchard plot analysis. The Scatchard equation is represented as follows (Equation (4)):

$$Q/[Template] = \frac{(Q_{max} - Q)}{K_D} \quad (4)$$

where  $Q$  is the amount of DTZ bound to the prepared biomaterials at equilibrium,  $Q_{max}$  is the apparent maximum number of binding sites,  $[Templates]$  is the free DTZ concentration at equilibrium and  $K_D$  is the equilibrium dissociation constant of the binding site.

Selectivity factor ( $\alpha$ ) of the DTZ-imprinted biomaterials is the value of DTZ, ASA, AAP, or SLD bound to the DTZ-imprinted biomaterials compared with that of the DTZ. The  $\alpha$  values were calculated by the following equation:

$$\alpha = \frac{Q_{(DTZ, ASA, AAP \text{ or } SLD)}}{Q_{DTZ}} \quad (5)$$

where  $Q_{(DTZ, ASA, AAP, \text{ OR } SLD)}$  is the adsorbed amount of DTZ, ASA, AAP, or SLD for DTZ-imprinted biomaterials and  $Q_{DTZ}$  is the adsorbed amount of DTZ for DTZ-imprinted biomaterials.

In addition, the imprinting effect was investigated with the imprinting-induced promotion of binding (IPB).<sup>19,20</sup> The IPB is evaluated by the following equation:

$$IPB = \frac{(Q_{Imprinting} - Q_{non-imprinting})}{Q_{non-imprinting}} \quad (6)$$

where  $Q_{Imprinting}$  is the adsorbed amount of DTZ, ASA, AAP, or SLD on DTZ-imprinted biomaterials and  $Q_{non-imprinting}$  is the corresponding value for non-imprinted biomaterials.

## 2.6 | DTZ release properties

The release behavior of DTZ from DTZ-imprinted CSA-based biomaterials under the influence of pH was confirmed using different pH buffers (pH 4.0, 7.0, and 10.0) at 36.5°C. The prepared biomaterials were immersed in a buffer (30 mL) and incubated in a shaking incubator at 50 rpm. At predetermined time points, the release medium was collected, and the released DTZ was analyzed using a UV-vis spectrophotometer at 236 nm. The cumulative amount of DTZ was calculated using a standard calibration curve. The applicability of DTZ-

imprinted CSA-based biomaterials as TDDS was evaluated via an artificial skin test (Neoderm-ED, Tego Science, Inc. Korea). Here, the prepared biomaterials (ca. 2.0 cm × 2.0 cm) were placed on artificial skin fixed in a medium containing agarose gel at 36.5°C and RH 60.0%. Afterward, the medium was immersed in DW at 25.0°C for 8 h.

To evaluate the DTZ release kinetics, Fickian diffusion, and Korsmeyer-Peppas models were employed. Fick's law can be used to determine the diffusion coefficient of a targeted drug in a polymer matrix (Equation (7)).<sup>21,22</sup>

$$\frac{\partial C}{\partial t} = D \frac{\partial^2 C}{\partial x^2} \quad (7)$$

where  $C$  is the concentration of the released DTZ at time  $t$  and  $D$  is the constant diffusion coefficient. The solution of Equation (7) is presented in the form of a trigonometric series and expressed in Equation (8), which is known as the Fickian diffusion model.<sup>23,24</sup>

$$\frac{M_t}{M_\infty} = 1 - \sum_{n=0}^{\infty} \frac{8}{(2n+1)^2 \pi^2} \exp \left[ -\frac{D_{eff} \cdot (2n+1)^2 \pi^2}{l^2} \cdot t \right] \quad (8)$$

where  $M_t$  is the amount of released DTZ at time  $t$ , and  $M_\infty$  is the amount of released DTZ at infinite time.  $l$ ,  $t$ , and  $D_{eff}$  are the half-thickness of the polymer matrix, diffusion time, and diffusion coefficient, respectively.

Drug release from polymeric systems can be simply described by the Korsmeyer-Peppas model (Equation (9)).<sup>25,26</sup>

$$\frac{M_t}{M_\infty} = kt^n \quad (9)$$

where  $k$  is the drug release constant, and  $n$  is a diffusional exponent. The values of  $n$  estimate the diffusion mechanism by which the drug is released into the surrounding medium as well as the extent to which the mechanisms depend on the shape of the system.  $n < 0.5$  corresponds to the pseudo-Fickian diffusion mechanism,  $n = 0.5$  indicates a Fickian diffusion mechanism, and  $0.5 < n < 1.0$  represents a non-Fickian diffusion mechanism.<sup>27</sup>

## 2.7 | Statistical analysis

All experiments were performed at least three times. The test results are reported as the mean ± standard



deviation. Statistical significance was confirmed via a *t*-test of the repeated experimental results.

### 3 | RESULTS AND DISCUSSION

#### 3.1 | Physical properties of CSA-based biomaterials

Improving the physical properties of natural polymer-based biomaterials significantly contributes to their applications in the field of biomedical engineering. Especially, water resistance properties can be a criterion to evaluate the crosslinking of constituents in the biomaterials. Figure 2a presents the water resistance properties of CSA-based biomaterials at various UV irradiation times. The increase in UV irradiation time rapidly decreased the swelling behavior (SB) and solubility (S) of the prepared biomaterials for 30 min. These results suggest that the crosslinking of the prepared biomaterials is enhanced,

thus increasing water resistance properties. However, when the UV irradiation time exceeded 30 min, the SB slightly decreased, while the S remained constant. Moreover, the prepared biomaterials underwent severe discoloration and oxidation. Based on these results, the CSA-based biomaterials were prepared under the condition of UV irradiation for 30 min.

In addition, Figure 2b shows the results of mechanical properties with UV irradiation time. From the results, it can be clearly confirmed that the mechanical properties were improved by UV irradiation. Figure 2c presents the mechanical properties of CSA-based biomaterials with DTZ, CA, and GL using UV irradiation for 30 min. The results confirmed that the tensile strength (TS) of GL- or CA-added biomaterials was lower and their elongation at break (EB) was higher than those of biomaterials without GL or CA. The functional groups in the plasticizers improve the flexibility of prepared biomaterials, which increases EB. However, the TS and EB of the biomaterials with/without the imprinted DTZ presented slight differences.

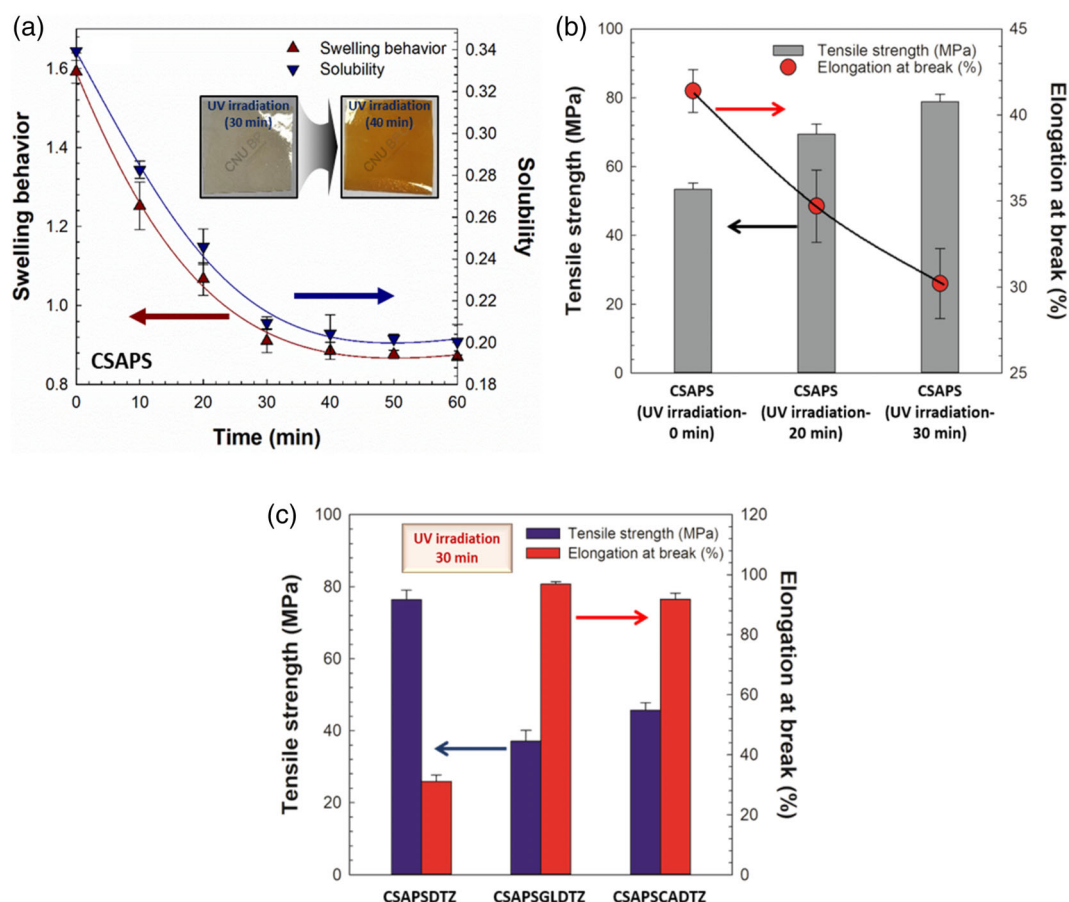


**FIGURE 2** Physical properties of CH based biomaterials with UV irradiation. (a) Water resistance properties of CSA based biomaterials with different UV irradiation times. (b) Mechanical properties of CSA based biomaterials with UV irradiation time. (b) Mechanical properties of CSA based biomaterials with DTZ and plasticizer using UV irradiation for 30 min. [Color figure can be viewed at [wileyonlinelibrary.com](https://onlinelibrary.wiley.com/doi/10.1002/app.56307)]

### 3.2 | Characterization

FE-SEM images of the surfaces and cross-sections of the prepared CSA-based biomaterials are shown in Figures 3a–e. These biomaterials with/without plasticizers and DTZ had a homogeneous morphology, and no cracks or pores were observed after UV irradiation.

FT-IR and  $^1\text{H}$  NMR analysis was performed to evaluate the stability of DTZ and prepared CSA-based biomaterials under UV irradiation. Figure 4a shows the FT-IR spectra of DTZ before/after UV irradiation. The peak of DTZ at  $2388\text{ cm}^{-1}$  is attributable to amine HCl stretching.<sup>27,28</sup> The sharp peaks at  $1741$ ,  $1678$ , and  $1216\text{ cm}^{-1}$  are related to ester C=O stretching, ketone C=O, and ether C-O, respectively.<sup>29,30</sup> Figure 4b presents the  $^1\text{H}$  NMR spectra of DTZ before/after UV irradiation. These results revealed peaks corresponding to the benzene ring at  $6.92$ – $7.79\text{ ppm}$  and those related to the methine group at  $4.99$  and  $5.14\text{ ppm}$ . In addition, peaks associated with the methyl group were found at  $1.82$ ,  $2.75$ , and  $3.77\text{ ppm}$ ; a peak assigned to the methylene group was observed at  $3.31\text{ ppm}$ .<sup>31</sup> The FT-IR and  $^1\text{H}$  NMR spectra of DTZ before/after UV irradiation were identical, confirming the absence of deformation in the structure of the UV-irradiated DTZ.

The FT-IR spectra of the prepared biomaterials are shown in Figure 4c. The peaks of C=O stretching in amide I at  $1628$ – $1635\text{ cm}^{-1}$ , those of N-H stretching

in amide II at  $1558$ – $1560\text{ cm}^{-1}$ , and those of C-O stretching at  $1030$ – $1039\text{ cm}^{-1}$  are confirmed in CSA.<sup>32,33</sup> The broad band at  $3308$ – $3319\text{ cm}^{-1}$  corresponds to stretching vibrations of -OH and the band at around  $2930$ – $2939\text{ cm}^{-1}$  is associated with aliphatic C-H stretching vibrations. The peak at  $1723$ – $1734\text{ cm}^{-1}$  is attributable to  $\text{COO}^-$  group vibrations.<sup>34,35</sup> These results indicate that DTZ-imprinted CSA-based biomaterials were successfully prepared without significant chemical interactions between DTZ and the biomaterials.

### 3.3 | DTZ recognition properties

Understanding the recognition properties of drug-imprinted biomaterials is important for the controlled release of targeted drugs and the quantitative analysis of optimal dosage. To evaluate the recognition properties of CSA-based biomaterials, adsorption isotherms and Scatchard plot analysis were performed by rebinding DTZ using the biomaterials from which DTZ was extracted. Figure 5a shows the DTZ extraction results of DTZ-imprinted CSA-based biomaterials with/without the addition of plasticizers. In the prepared biomaterials, more than 99% of DTZ was extracted in 28 h and at  $25.0^\circ\text{C}$ , with slight differences in the extraction ratio (%) depending on the type of plasticizers. The results of the binding isotherms and Scatchard plot for DTZ in the

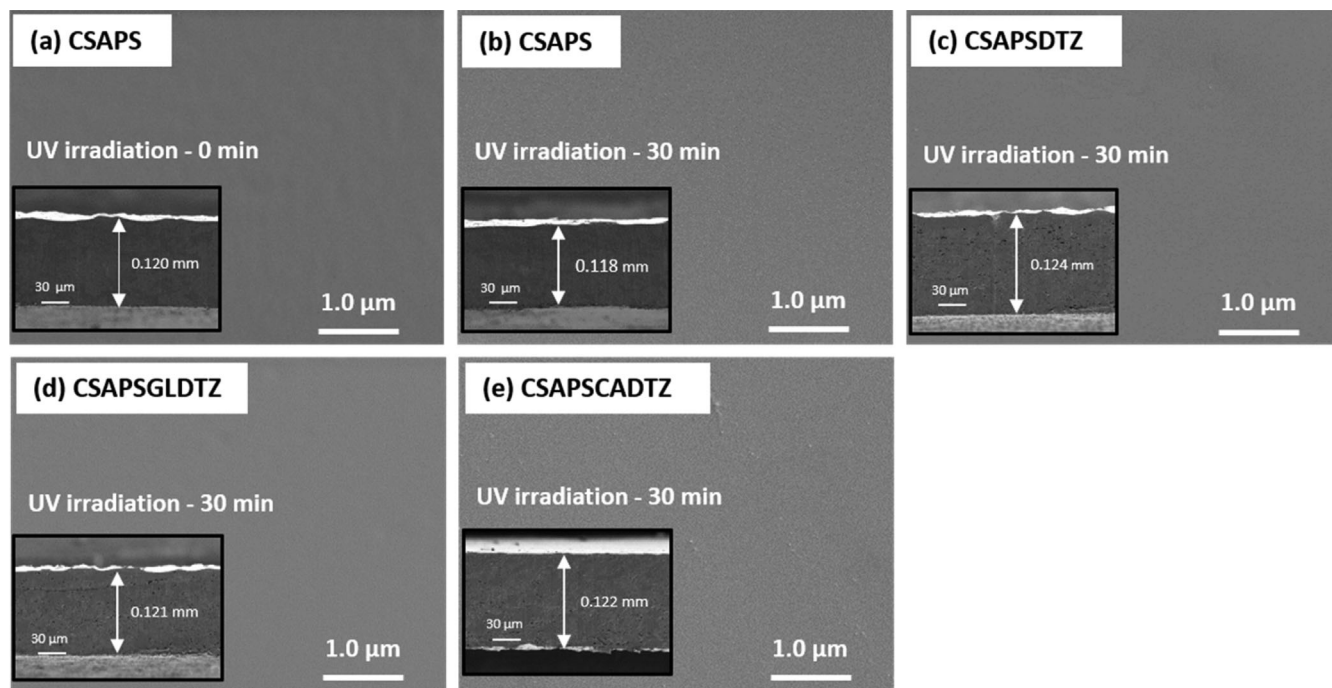


**FIGURE 3** FE-SEM images of surface and cross-section of CSA-based biomaterials. (a) CSA-based biomaterials. (b) CSA-based biomaterials using UV irradiation. (c) DTZ-imprinted CSA-based biomaterials using UV irradiation. (d) DTZ-imprinted CSA-based biomaterials with GL using UV irradiation. (e) DTZ-imprinted CSA-based biomaterials with CA using UV irradiation.

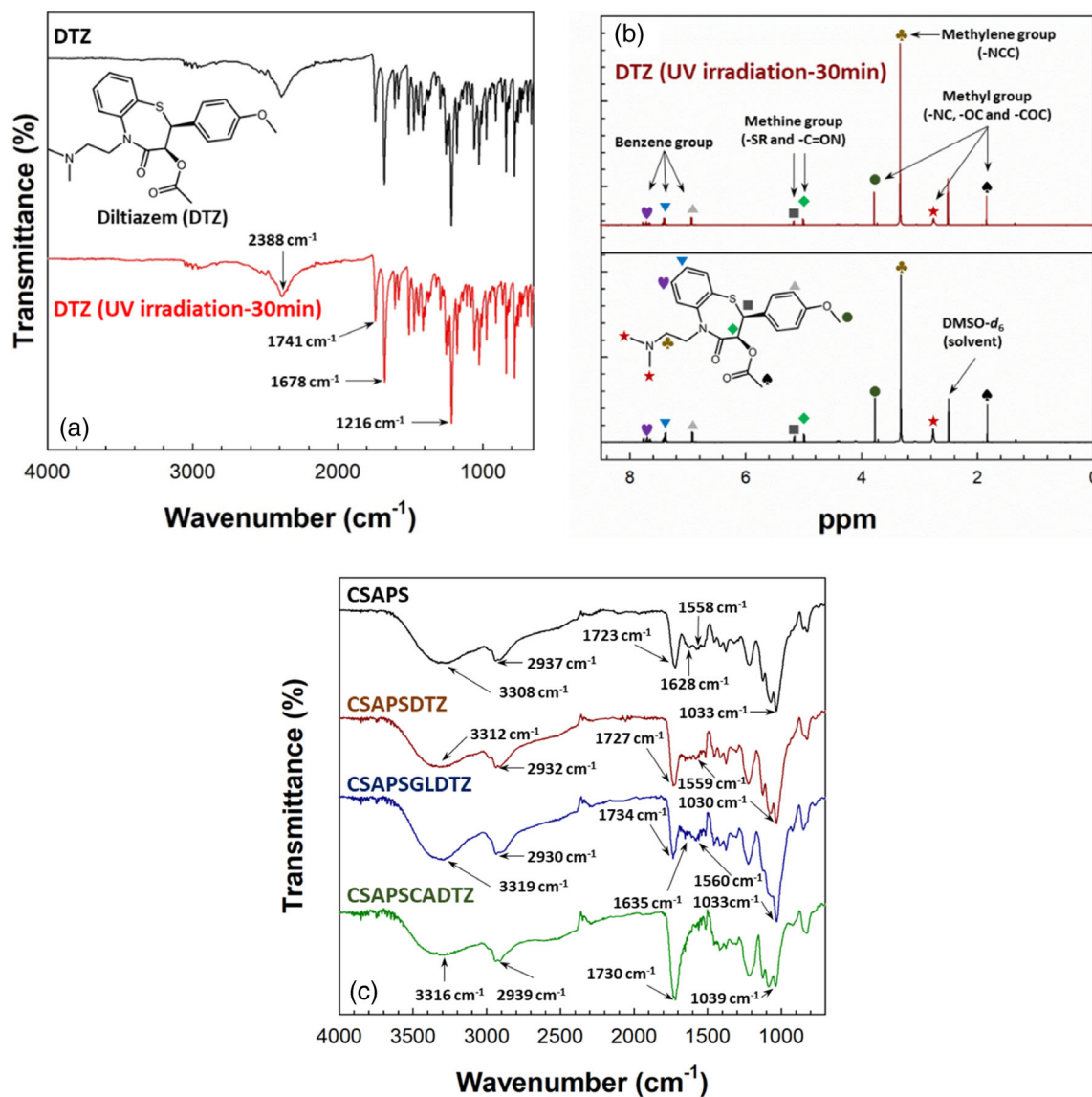


**FIGURE 4** (a) FT-IR spectra of DTZ with/without UV irradiation. (b) <sup>1</sup>H NMR spectra of DTZ with/without UV irradiation. (c) FT-IR spectra of CSA-based biomaterials with/without DTZ and plasticizers using UV irradiation. [Color figure can be viewed at [wileyonlinelibrary.com](https://onlinelibrary.wiley.com/doi/10.1002/app.56307)]

prepared biomaterials are shown in Figures 5b,c. The  $Q$  of the prepared biomaterials gradually increased with the increasing concentration of DTZ. Owing to the effect of DTZ-imprinted biomaterials on DTZ recognition, their  $Q$  was 1.63–2.53 times higher than that of non-imprinted biomaterials. The results also indicated differences in the  $Q$  of DTZ-imprinted biomaterials depending on the type of plasticizer added, and the  $Q$  of the CA-added biomaterials was higher than that of the GL-added biomaterials. These results are explained by the influence of the functional groups of the plasticizers. In contrast to GL with only hydroxyl groups, CA with carboxyl and hydroxyl groups can form more binding sites for the adsorption of DTZ inside the biomaterials.

The binding site and affinity of these biomaterials for the target drug are confirmed by Scatchard plot analysis.

The results identified two distinct sections within the plot that could be regarded as straight lines. These two lines imply that there are two kinds of binding sites on DTZ-imprinted biomaterials. On the other hand, only one straight line was observed for non-imprinted biomaterials. The steeper and flatter lines are associated with the high affinity sites (specific binding sites) and the low affinity sites (non-specific binding sites), respectively.<sup>36</sup> The Equation (4) can be redefined as follows:

$$Q/[Template] = \frac{(Q_{max1} - Q_1)}{K_{D1}} + \frac{(Q_{max2} - Q_2)}{K_{D2}} \quad (10)$$

where  $Q_1$ ,  $Q_{max1}$ , and  $K_{D1}$  describe the high affinity sites, whereas  $Q_2$ ,  $Q_{max2}$ , and  $K_{D2}$  correspond to the low affinity sites.



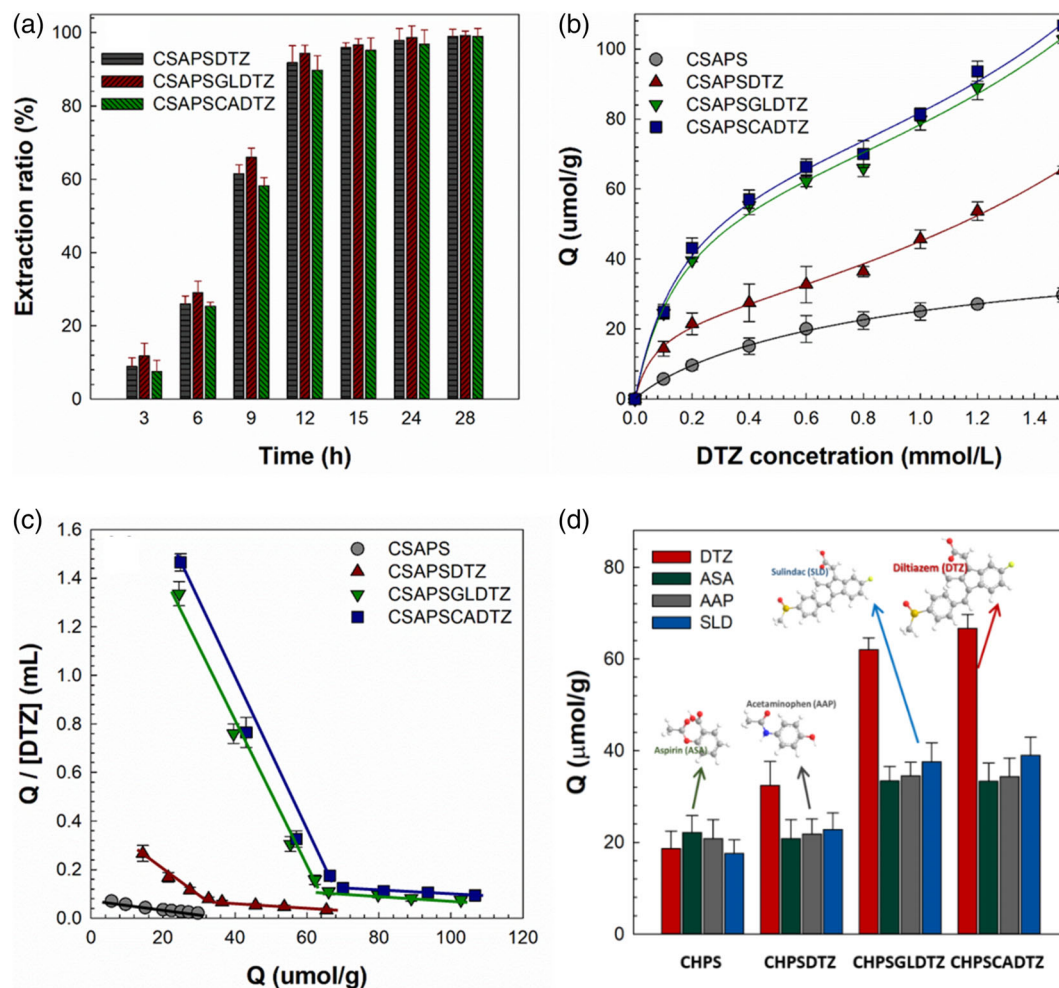


**FIGURE 5** Recognition properties of CSA-based biomaterials. (a) The extraction ratio (%) of DTZ into DTZ-imprinted CSA-based biomaterials. (b) Binding isotherm of DTZ-imprinted CSA-based biomaterials. (c) Scatchard plot analysis of DTZ-imprinted CSA-based biomaterials. (d) Adsorbed amount ( $Q$ ) of DTZ, ASA, AAP, and SLD on DTZ-imprinted CSA-based biomaterials and non-imprinted CSA-based biomaterials. [Color figure can be viewed at [wileyonlinelibrary.com](https://onlinelibrary.wiley.com/doi/10.1002/app.56307)]

**TABLE 2**  $K_D$  and  $Q_{max}$  were calculated from the slope and intercept of the Scatchard plot.

Sample name	$K_{D2}$ (μmol/g)	$K_{D2}$ (μmol/g)	$K_D$ (μmol/g)	$Q_{max1}$ (μmol/L)	$Q_{max2}$ (μmol/L)	$Q_{max}$ (μmol/L)
CSAPSDTZ	98.039	909.091	1007.130	39.392	96.818	136.210
CSAPSGLDTZ	31.949	1000.000	1031.949	65.875	162.000	227.875
CSAPSCADTZ	31.446	1250.000	1281.446	69.299	222.625	291.924

The equilibrium dissociation constants ( $k$ ) and maximum apparent numbers ( $Q_{max}$ ) calculated using Equation (10) are found in Table 2. The  $Q_{max}$  values indicated a difference depending on the plasticizer added to the biomaterials, and the  $Q_{max}$  of CSAPSCADTZ (291.924 μmol/L) had the highest value. These results indicate that CSAPSCADTZ has the most binding sites. Therefore, CSAPSCADTZ can adsorb the most DTZ, as confirmed in Figure 5b, indicating its excellent recognition ability for DTZ. In previous study,<sup>37</sup> we reported on the recognition properties for the prepared SLD-

imprinted starch-based biomaterials, which were investigated by the binding isotherm and Scatchard plot analysis. Results indicated that the recognition ability of CSA-based biomaterials prepared to this study is superior to that of starch-based biomaterials. Consequently, CSA-based materials with compact structures are judged to be more effective than starch-based materials. As the results of Table 3, we can clearly find that the prepared DTZ-imprinted biomaterials have recognition capabilities according to the  $\alpha$  and IPB values. From the results of  $\alpha$  values, we verified that the  $\alpha$  values of DTZ-imprinted

TABLE 3 Selectivity factor ( $\alpha$ ) and the imprinting-induced promotion of binding (IPB) for DTZ-imprinted CSA-based biomaterials.

	Selectivity factor ( $\alpha$ )				IPB		
	CSAPS-DTZ	CSAPSGL-DTZ	CSAPSCA-DTZ	CSAPS	CSAPS-DTZ	CSAPSGL-DTZ	CSAPSCA-DTZ
DTZ	1	1	1	—	0.7409	2.3275	2.5762
ASA	0.6422	0.5385	0.5006	—	−0.059	0.5082	0.5067
AAP	0.6728	0.5562	0.5160	—	0.047	0.6552	0.6491
SLD	0.7034	0.6061	0.5850	—	0.2977	1.137	1.2174

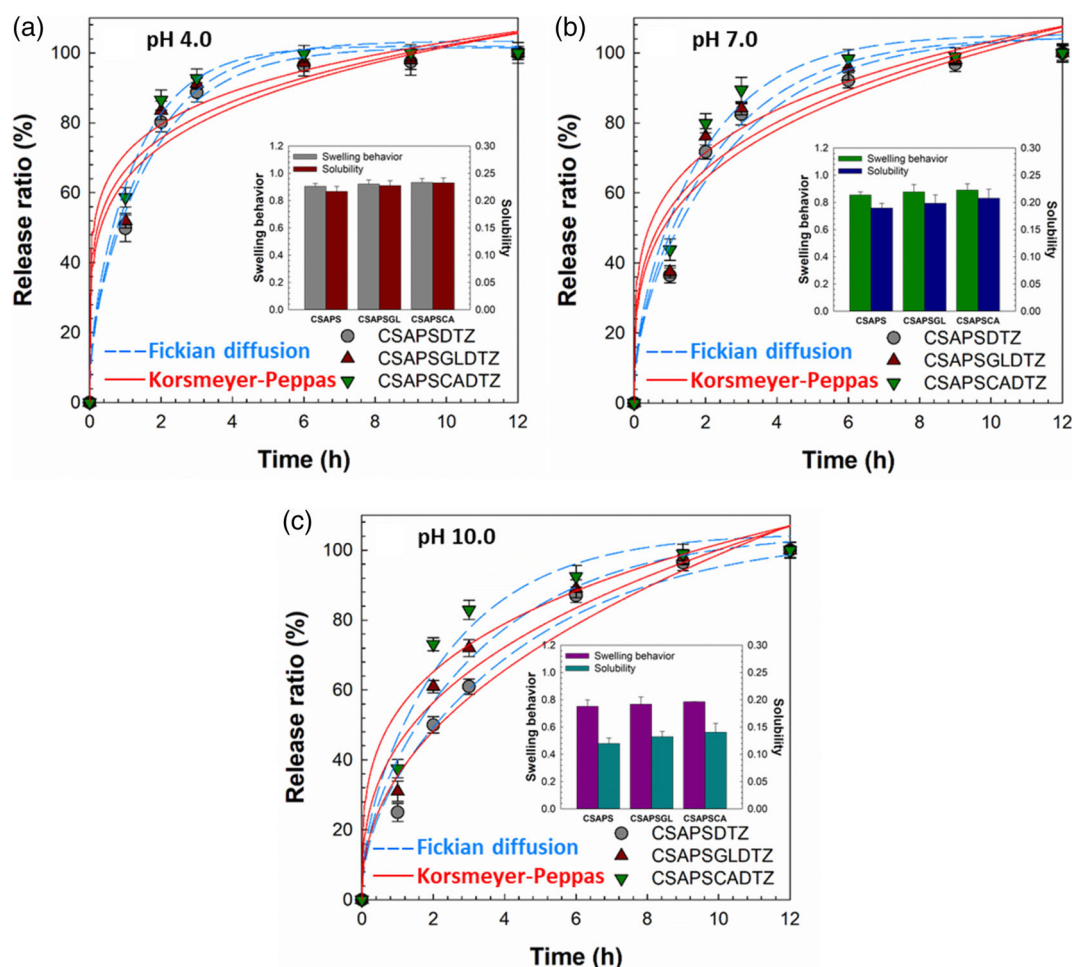


FIGURE 6 Release properties of DTZ-imprinted CSA-based biomaterials at various pH buffers and 36.5°C. The symbols represent the DTZ release behavior, and the long dash and solid lines depict the Fickian diffusion and Korsmeyer-Peppas model fitting, respectively. Insets indicate SB and S of CSA-based biomaterials with/without plasticizers at various pH buffers. [Color figure can be viewed at [wileyonlinelibrary.com](https://onlinelibrary.wiley.com/doi/10.1002/app.56397)]

biomaterials were smaller than 1 when materials that were structurally similar to DTZ were adsorbed on them. The IPB is a value that provides the imprinting efficiency more accurately than the  $Q$  values of target molecule imprinted biomaterials themselves. IPB value on DTZ-imprinted biomaterials was 2.0–3.8 times higher than the other values. However, in the case of SLD, results indicated that the  $\alpha$  and IPB values were relatively higher than those of ASA and AAP because of the similarity of

structure of DTZ. These results suggest that the prepared DTZ-imprinted biomaterials have molecule recognition capabilities.

### 3.4 | DTZ release properties

The DTZ release behavior of DTZ-imprinted CSA-based biomaterials was verified for their application to TDDS.

TABLE 4 Fickian diffusion and Korsmeyer-Peppas model parameters of DTZ release from DTZ-imprinted CSA-based biomaterials at various pH buffers and 36.5°C.

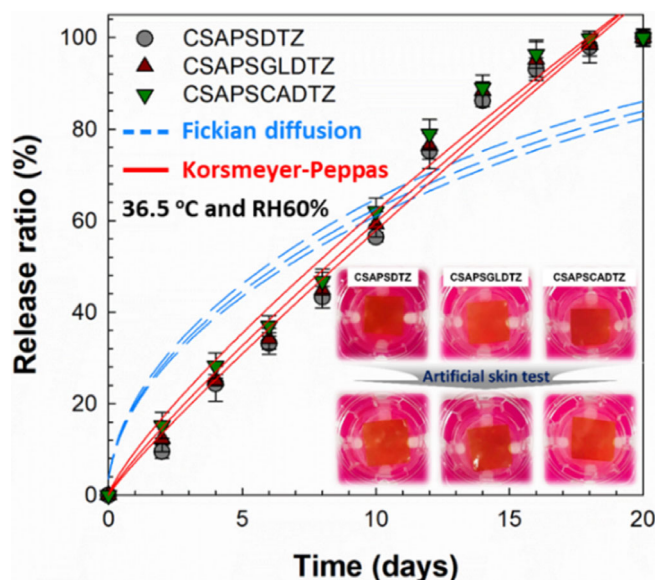
Fickian diffusion model										
CSAPSDTZ					CSAPSGLDTZ					
pH	4.0	7.0	10.0		4.0	7.0	10.0	4.0	7.0	10.0
$M_{\infty}$	101.655	105.266	105.300		103.402	104.681	105.275	101.972	105.358	104.903
$D_{eff}$	7.903, E-10	5.029, E-10	3.007, E-10		8.343, E-10	5.755, E-10	3.966, E-10	1.022, E-9	6.796, E-10	5.339, E-10
$R^2$	0.989	0.970	0.982		0.985	0.969	0.984	0.994	0.975	0.973
Korsmeyer-Peppas model										
CSAPSDTZ					CSAPSGLDTZ					
pH	4.0	7.0	10.0		4.0	7.0	10.0	4.0	7.0	10.0
$M_{\infty}$	596.492	562.551	492.540		604.238	569.444	529.765	616.079	586.067	564.512
$k$	0.106	0.0940	0.0720		0.110	0.0975	0.0832	0.115	0.104	0.0954
$n$	0.204	0.281	0.445		0.187	0.265	0.356	0.161	0.228	0.276
$R^2$	0.853	0.839	0.871		0.849	0.828	0.862	0.860	0.831	0.841

Figure 6 presents the DTZ release ratio of prepared biomaterials with/without plasticizers at various pH buffers and 36.5°C. DTZ was rapidly released until 6 h and more than 98% of it was released within 12 h. Moreover, DTZ release at low pH was faster than that at high pH, indicating the water resistance properties of the biomaterials at different pH levels (see inset of Figure 6). Because the solubility of CSA increases at low pH, the intermolecular interactions of CSA-based biomaterials are weakened; thus, DTZ inside the biomaterials is released into the release medium relatively quickly. The DTZ release behavior was found to vary based on the type of plasticizers added to the biomaterials in the following order: CSAPSCADTZ > CSAPSGLDTZ > CSAPSDTZ. These results are obtained because the plasticizers used in the biomaterials have high solubility. In particular, CA reduces the pH after dissolution in buffers, leading to a rapid release of DTZ from the prepared biomaterials.

Figure 6 and Table 4 show the results of using mathematical models to investigate the DTZ release behavior of prepared biomaterials in various pH buffers and at 36.5°C. These results confirm that the Fickian diffusion model ( $R^2 = 0.969\text{--}0.994$ ) predicts more satisfactorily than the Korsmeyer-Peppas model ( $R^2 = 0.828\text{--}0.871$ ). The  $D_{eff}$  values of prepared biomaterials increased with decreasing pH levels; the DTZ release of CSAPSCADTZ at pH 4.0 was found to have the highest  $D_{eff}$  value (1.022E-9), whereas the DTZ release of CSAPSDTZ at pH 10.0 was found to have the lowest  $D_{eff}$  value (3.007E-10). Korsmeyer-Peppas model parameters revealed that the  $n$  values of DTZ-imprinted biomaterials were less than 0.5. These results reveal that DTZ release properties at various pH level buffers followed a pseudo-Fickian diffusion mechanism.

### 3.5 | DTZ release properties using artificial skin

To determine the applicability of the DTZ-imprinted CSA-based biomaterials as a TDDS, their DTZ release properties were investigated using an artificial skin test at RH 60% and 36.5°C. Figure 7 indicates the DTZ release profiles of the prepared biomaterials with/without plasticizers using artificial skin. The results indicate that the DTZ release ratio (%) increased at a relatively steady-state rate with increasing test time for 20 days. The cumulative concentration of DTZ was slightly different depending on the type of plasticizers added to the biomaterials, similar to the DTZ release behavior in various pH buffers.



**FIGURE 7** Release properties of DTZ-imprinted CSA-based biomaterials using artificial skin test at 36.5°C and RH 60%. The symbols represent the DTZ release behavior, and the long dash and solid lines depict the Fickian diffusion and Korsmeyer-Peppas model fitting, respectively. [Color figure can be viewed at [wileyonlinelibrary.com](https://onlinelibrary.wiley.com)]

**TABLE 5** Fickian diffusion and Korsmeyer-Peppas model parameters of DTZ release from DTZ-imprinted CSA-based biomaterials using artificial skin test at 36.5°C and RH 60%.

Fickian diffusion model			
	CSAPSDTZ	CSAPSGLDTZ	CSAPSCADTZ
$M_{\infty}$	105.225	105.338	105.479
$D_{\text{eff}}$	9.283E-11	9.772E-11	1.047E-10
$R^2$	0.837	0.847	0.864
Korsmeyer-Peppas model			
	CSAPSDTZ	CSAPSGLDTZ	CSAPSCADTZ
$M_{\infty}$	107.042	112.002	120.269
$k$	0.0669	0.0717	0.0794
$n$	0.907	0.871	0.814

The simulation results of the mathematical models to explain the DTZ release mechanism in the artificial skin test are presented in Figure 7 and Table 5. The  $R^2$  of the mathematical models indicates that the fitting of the Korsmeyer-Peppas model is more appropriate than that of the Fickian diffusion model. Furthermore, because the  $n$  values of the parameters in the Korsmeyer-Peppas model were 0.814, 0.871, and 0.907, the DTZ release profile of prepared biomaterials using artificial skin followed a non-Fickian diffusion mechanism.

## 4 | CONCLUSIONS

The oral administration of DTZ leads to its low bioavailability and short biological half-life. Thus, we prepared DTZ-imprinted biomaterials using CSA, PVA, SSA, and plasticizers (GL and CA) for the transdermal administration of DTZ. The optimal UV irradiation time was set by evaluating the water resistance properties of CSA-based biomaterials with various UV irradiation times. In addition, the stability of DTZ against UV irradiation was analyzed by FT-IR and  $^1\text{H}$  NMR spectroscopy. The morphology and molecular structures of the prepared biomaterials were also characterized using FE-SEM and FT-IR. The DTZ recognition capabilities of the DTZ-imprinted biomaterials were assessed by the binding isotherm, Scatchard plot analysis, the adsorption of materials with structures similar to DTZ (ASA, AAP, and SLD),  $\alpha$ , and IPB. The results confirmed that the  $Q$  of DTZ-imprinted biomaterials was 1.63–2.53 times higher than that of non-imprinted biomaterials. The results of Scatchard plot analysis also revealed two classes of binding sites in DTZ-imprinted biomaterials. The DTZ-imprinted biomaterials were confirmed to have relatively high  $\alpha$  and IPB values for DTZ, indicating the molecular recognition ability of the prepared DTZ-imprinted biomaterials for DTZ as a target drug. The evaluation of the release properties in various pH buffers revealed that over 98% of the DTZ of the prepared biomaterials was released into the release medium within 12 h, and the DTZ release rate at low pH levels was faster than that at high pH levels. The DTZ release behavior at various pH levels was also described by the Fickian diffusion model and followed a pseudo-Fickian diffusion mechanism. Investigations of the DTZ release properties using the artificial skin test revealed that DTZ was sustainably released for 20 days. Moreover, the DTZ release profile in artificial skin was more suitably fitted by the Korsmeyer-Peppas model and evaluated to follow a non-Fickian diffusion mechanism.

## AUTHOR CONTRIBUTIONS

**Kyeong-Jung Kim:** Formal analysis (equal); methodology (equal); software (supporting); validation (equal); visualization (lead). **Ji-Hoon Kang:** Formal analysis (equal); investigation (equal); software (equal); validation (supporting). **Se-woon Choe:** Data curation (equal); formal analysis (lead); methodology (equal); software (lead); validation (lead). **Yeon-Hum Yun:** Conceptualization (equal); formal analysis (lead); investigation (equal); methodology (equal); resources (equal). **Soon-Do Yoon:** Conceptualization (lead); formal analysis (lead); funding acquisition (lead); methodology (lead); project administration (lead); resources (equal); supervision (lead);



validation (lead); writing – original draft (lead); writing – review and editing (lead).

## ACKNOWLEDGMENTS

This research was supported by Basic Science Research Program through the National Research Foundation of Korea (NRF) funded by the Ministry of Education (Grant no. NRF-2019R1I1A3A01061508).

## DATA AVAILABILITY STATEMENT

Data supporting the findings of this study are available from the corresponding author upon reasonable request.

## ORCID

Soon-Do Yoon  <https://orcid.org/0000-0002-3519-3071>

## REFERENCES

- [1] M. R. Prausnitz, R. Langer, *Nat. Biotechnol.* **2008**, 26, 1261.
- [2] P. K. Kiptoo, M. O. Hamad, P. A. Crooks, A. L. Stinchcomb, *J. Controlled Release* **2006**, 113, 137.
- [3] R. M. Galzote, S. Rafie, R. Teal, S. K. Mody, *Int. J. Womens Health* **2017**, 9, 315.
- [4] F. Sabbagh, B. S. Kim, *J. Controlled Release* **2022**, 341, 132.
- [5] S. Rashki, K. Asgarpour, H. Tarrahimofrad, M. Hashemipour, M. S. Ebrahimi, H. Fathizadeh, A. Khorshidi, H. Khan, Z. Marzhoseyni, M. S. Niasari, H. Mirzaei, *Carbohydr. Polym.* **2021**, 251, 117108.
- [6] F. Ahmed, F. M. Soliman, M. A. Adly, H. A. M. Soliman, M. E. Matbouli, M. Saleh, *Res. Vet. Sci.* **2019**, 126, 68.
- [7] H. Hamed, S. Moradi, S. M. Hudson, A. E. Tonelli, M. W. King, *Carbohydr. Polym.* **2022**, 282, 119100.
- [8] H. Wang, J. Qian, F. Ding, *J. Agric. Food Chem.* **2018**, 66, 395.
- [9] M. A. Pigaleva, I. V. Portnov, A. A. Rudov, I. V. Blagodatskikh, T. E. Grigoriev, M. O. Gallyamov, I. I. Potemkin, *Macromolecules* **2014**, 47, 5749.
- [10] H. Wang, R. Zhang, H. Zhang, S. Jiang, H. Liu, M. Sun, S. Jiang, *Carbohydr. Polym.* **2015**, 127, 64.
- [11] C. H. Chen, F. Y. Wang, C. F. Mao, C. H. Yang, *J. Appl. Polym. Sci.* **2007**, 105, 1086.
- [12] J. S. Park, J. W. Park, E. Ruckenstein, *Polymer* **2001**, 42, 4271.
- [13] Y. H. Yun, C. M. Lee, Y. S. Kim, S. D. Yoon, *Food Res. Int.* **2017**, 100, 377.
- [14] J. Jegal, K. H. Lee, *J. Appl. Polym. Sci.* **1999**, 71, 671.
- [15] S. E. O'Connor, A. Grosset, P. Janiak, *Fundam. Clin. Pharmacol.* **1999**, 13, 145.
- [16] G. H. O. Paula, S. C. Pereira, J. E. T. Santos, R. Lacchini, *Pharmacogn. Pers. Med.* **2019**, 12, 341.
- [17] G. Sarkar, N. R. Saha, I. Roy, A. Bhattacharyya, M. Bose, R. Mishra, D. Rama, D. Bhattacharjee, D. Chattopadhyay, *Int. J. Biol. Macromol.* **2014**, 66, 158.
- [18] E. Limpongsa, K. Umprayn, *AAPS PharmSciTech* **2008**, 9, 64.
- [19] T. Hishiya, M. Shibata, M. Kakazu, H. Asanuma, M. Komiyama, *Macromolecules* **1999**, 32, 2265.
- [20] H. S. Byun, Y. N. Youn, Y. H. Yun, S. D. Yoon, *Sep. Purif. Technol.* **2010**, 74, 144.
- [21] V. D. Paramita, A. Bannikova, S. Kasapis, *Carbohydr. Polym.* **2015**, 126, 141.
- [22] B. Watts, W. J. Belcher, L. Thomsen, H. Ade, P. C. Dastoor, *Macromolecules* **2009**, 42, 8392.
- [23] K. J. Kim, Y. H. Yun, J. Y. Je, D. H. Kim, H. S. Hwang, S. D. Yoon, *Process Biochem.* **2023**, 129, 268.
- [24] P. L. Ritger, N. A. Peppas, *J. Controlled Release* **1987**, 5, 23.
- [25] A. Plichta, S. Kowalczyk, K. Kamiński, M. Wasyleczko, S. Więckowski, E. Oledzka, G. N. Jawecki, A. Zgadzaj, M. Sobczak, *Macromolecules* **2017**, 50, 6437.
- [26] S. Bohrey, V. Chourasiya, A. Pandey, *Nano Converg.* **2016**, 3, 1.
- [27] P. Costa, J. M. S. Lobo, *Eur. J. Pharm. Sci.* **2001**, 13, 123.
- [28] T. S. Anirudhan, A. S. Nair, S. S. Gopika, *Int. J. Biol. Macromol.* **2018**, 107, 779.
- [29] R. Parhi, P. Suresh, *J. Adv. Res.* **2016**, 7, 539.
- [30] R. V. Kulkarni, B. S. Mangond, S. Mutalik, B. Sa, *Carbohydr. Polym.* **2011**, 83, 1001.
- [31] D. Stepaniv, M. Jure, M. Gosteva, J. Popelis, G. Kiselovs, A. Mishnev, *CrystEngComm* **2016**, 18, 1235.
- [32] D. Hu, L. Wang, *Mater. Res. Bull.* **2016**, 78, 46.
- [33] I. Leceta, P. Guerrero, I. Ibarburu, M. T. Dueñas, K. Caba, *J. Food Eng.* **2013**, 116, 889.
- [34] G. Ma, D. Yang, Y. Zhou, M. Xiao, J. F. Kennedy, J. Nie, *Carbohydr. Polym.* **2008**, 74, 121.
- [35] S. Y. Lee, Y. H. Yun, G. Ahn, S. D. Yoon, *Int. J. Biol. Macromol.* **2023**, 232, 123382.
- [36] X. Liu, L. Zhu, X. Gao, Y. Wang, H. Lu, Y. Tang, J. Li, *Food Chem.* **2016**, 202, 309.
- [37] H. Y. Tak, Y. H. Yun, C. M. Lee, S. D. Yoon, *Carbohydr. Polym.* **2019**, 208, 261.

**How to cite this article:** K.-J. Kim, J.-H. Kang, S. Choe, Y.-H. Yun, S.-D. Yoon, *J. Appl. Polym. Sci.* **2024**, e56307. <https://doi.org/10.1002/app.56307>